

Effect of Processing Techniques on Precipitation Behavior of Secondary Phase Particles in Zr-1Nb-0.01Cu Alloy

Bai Guanghai^{1,2}, Wang Rongshan¹, Zhang Yanwei¹, Mei Jinna¹, Li Jinshan²,
Xue Xiangyi²

¹ Suzhou Nuclear Power Research Institute, Suzhou 215004, China; ² State Key Laboratory of Solidification Processing, Northwestern Polytechnical University, Xi'an 710072, China

Abstract: The precipitation behavior of secondary phase particles (SPPs) was investigated in Zr-1Nb-0.01Cu alloy prepared by various processing techniques. The results show that with the decrease of cold rolling and annealing steps, intermediate annealing temperatures, final annealing temperatures and time, the average sizes of SPPs decrease accordingly. The β -Zr phase formed at the intermediate annealing temperature (higher than 640 °C) is hard to dissolve in the matrix after final annealing treatment. During the long-time final annealing process, the SPPs with smaller size coalesce into larger particles by diffusion through the matrix gradually because of Ostwald ripening mechanism. It shows that the decrease of intermediate annealing temperature is more effective than other processing techniques for minimizing the size of SPPs. The average particle size smaller than 50 nm can be achieved by low intermediate/final annealing temperature (≤ 520 °C) or short annealing time (≤ 2 h) treatment. The investigations in the present paper are very meaningful to control the SPPs in Zr-Nb based alloys.

Key words: Zr-1Nb-0.01Cu alloy; processing technology; secondary phase particle; precipitation behavior; particle size

Zirconium alloys are used widely in pressurized water reactors (PWR) as fuel clads materials for their very low absorption cross-section of thermal neutrons, high strength, and excellent corrosion resistance^[1]. It is well known that corrosion resistance of zirconium alloys is seriously affected by microstructures, especially by SPPs^[2-4]. Researches indicate that for Zr-Nb and Zr-Sn-Nb based alloy, finer SPPs with the size smaller than 100 nm can improve corrosion resistance obviously^[2,5,6]. The mechanical properties of the alloys are also partly determined by the size and distribution of SPPs^[6]. Therefore, the SPPs in zirconium alloys play an important role in corrosion resistance and mechanical properties and it is necessary to understand their precipitation behavior.

Much attention has been focused on the SPPs precipitation behavior in zirconium alloys, and the results show that the precipitation behavior of SPPs are seriously

influenced by processing techniques^[7-11]. The related studies indicate that the intermediate and final annealing treatment has very important effects on the SPPs precipitation^[3,8]. Kim et al pointed out that the average size of SPPs in Zr-Nb-Cu alloy decreases with the decreasing annealing temperatures^[8]. The SPPs would precipitate dispersively in the matrix when the alloy is pre-deformed before final annealing treatment^[2,6]. Hence, it can be known that the precipitation behavior of SPPs in zirconium alloy is very complex, and it can be affected by various processing techniques. Up to now, there is little report about the comparison of the effect of processing techniques on SPPs precipitation behavior in zirconium alloys. In order to optimize the processing techniques and to get a good microstructure of zirconium alloys, it is necessary to pay more attention to the difference of the effects.

Recently, much effort has been devoted to develop

Received date: October 10, 2015

Foundation item: Suzhou Nuclear Power Research Institute Postdoctoral Sustentation Fund (2012)

Corresponding author: Bai Guanghai, Ph. D. Postdoctor, Suzhou Nuclear Power Research Institute, Suzhou 215004, P. R. China, Tel: 0086-512-68701561, E-mail: baiguanghai@foxmail.com

Copyright © 2016, Northwest Institute for Nonferrous Metal Research. Published by Elsevier BV. All rights reserved.

Zr-Nb-Cu alloy as potential fuel clad material^[8,9]. The SPPs precipitation behavior of the alloy has not been investigated systematically. In the present paper, systematic studies were done to study the effect of various processing techniques on the SPPs precipitation behavior of Zr-1Nb-0.01Cu alloy, and the difference was also discussed.

1 Experiment

The nominal chemical composition (wt%) of the experimental alloy is as follows: Nb 1, Cu 0.01, Zr Bal. The alloy ingot was cast by vacuum arc melting, and then it was β -quenched at 1020 °C, hot-forged and hot-rolled into a 10mm thick plate. In order to get a homogeneous microstructure and study the effect of processing techniques on SPPs precipitation behavior, the plate was annealed at 1020 °C for 20 min and then β -quenched again. The subsequent manufacture processes and technical parameters of the alloy are shown in Table 1 and Fig.1, Fig.1 includes cold rolling and annealing (hereinafter called as cold rolling) steps from 2 to 4, intermediate annealing temperatures 520, 580, 640, 700 °C, final annealing temperatures 460, 520, 560, 640 °C, and final annealing time 2, 4, 6, 8 h. Fig.1b gives the example of preparation process, which is corresponding to the craft B, E, N, I as shown in Fig.1a. To avoid being oxidized by air, specimens were sealed in evacuated quartz capsules at about 5×10^{-3} Pa.

The SPPs analysis of the alloy sample was performed on transmission electron microscopy (TEM) equipped with energy dispersive spectra (EDS). Photoshop CS4 and Image-Pro Plus 5.0 were used to get statistical information of SPPs size, with at least 200 particles counted for each specimen.

2 Results and Discussion

2.1 Effect of cold rolling steps on SPPs precipitation behavior

TEM microstructure analysis of Zr-1Nb-0.01Cu alloy cold rolled by 2 to 4 steps is shown in Fig.2a to 2e, and the corresponding processing techniques are shown in Table 1. The SPPs in the alloy are identified by analyzing the selected area electron diffraction (SAED) patterns, and the chemical compositions obtained by EDS results. It can be seen in Fig.2, that recrystallization is completed after aging at 560 °C for 4h. The α -Zr matrix shows an equiaxed grain structure, and a few dislocations are observed in the matrix. The SPPs precipitate randomly in the matrix, most of which distribute in the grains (Fig.2a, 2b, 2c). Studies show that the precipitation of SPPs always occurs earlier than the initiation of recrystallization during annealing treatment^[10,11]; as a result, the distribution and growth behavior of SPPs would be affected by the recrystallization process of the matrix.

SAED pattern (Fig.2d, 2e) and EDS analyses (Fig.2b) of SPPs show that there are two types of precipitates in the alloy: β -Nb phase which mainly contains Nb, Zr, Cu elements, and Zr-Nb-Fe particles which mainly contains Zr, Nb, Fe, Cr elements. Fe and Cr elements as impurity elements which are inevitable in a sponge Zr would be responsible for the formation of Fe, Cr-containing precipitates^[12]. The β -Nb particles are more frequently observed compared with Zr-Nb-Fe particles in the alloy. The research suggests that the maximum solubility

Table 1 Manufacture processes for Zr-1Nb-0.01Cu alloy

Figure	Craft	Figure	Craft	Figure	Craft
Fig.2a	A-E-N-I	Fig.3c	B-F-N-I	Fig.4d	B-E-O-I
Fig.2b	B-E-N-I	Fig.3d	B-G-N-I	Fig.5a	B-E-N-H
Fig.2c	C-E-N-I	Fig.4a	B-E-L-I	Fig.5c	B-E-N-J
Fig.3a	B-D-N-I	Fig.4b	B-E-M-I	Fig.5d	B-E-N-K

Note: the letters of “A” to “O” are explained in Fig.1

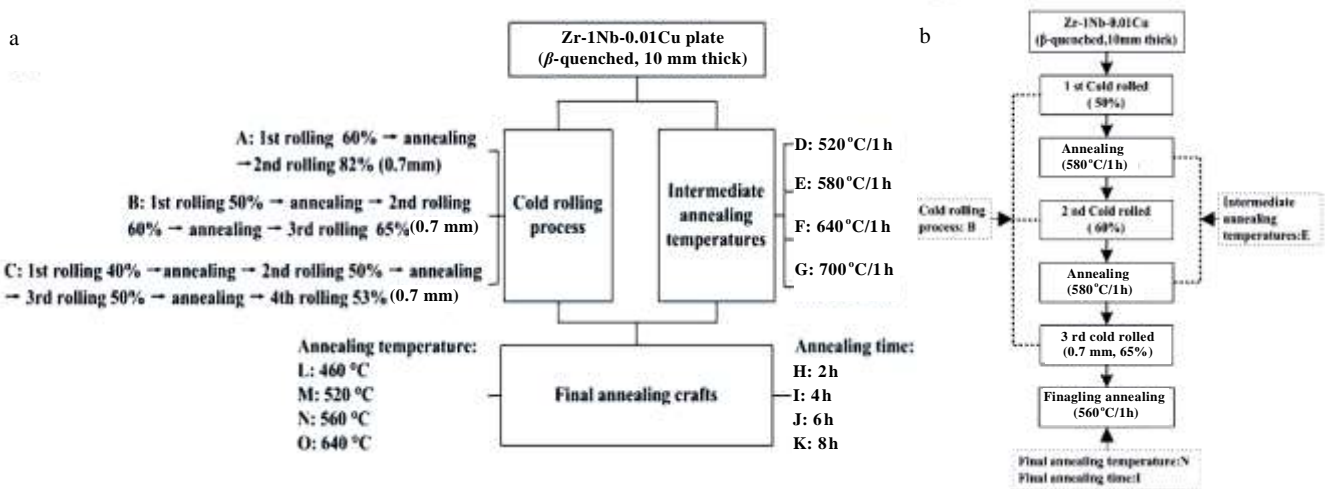


Fig.1 Zr-1Nb-0.01Cu alloy by various processing techniques (a); typical manufacturing process of the alloy (b)

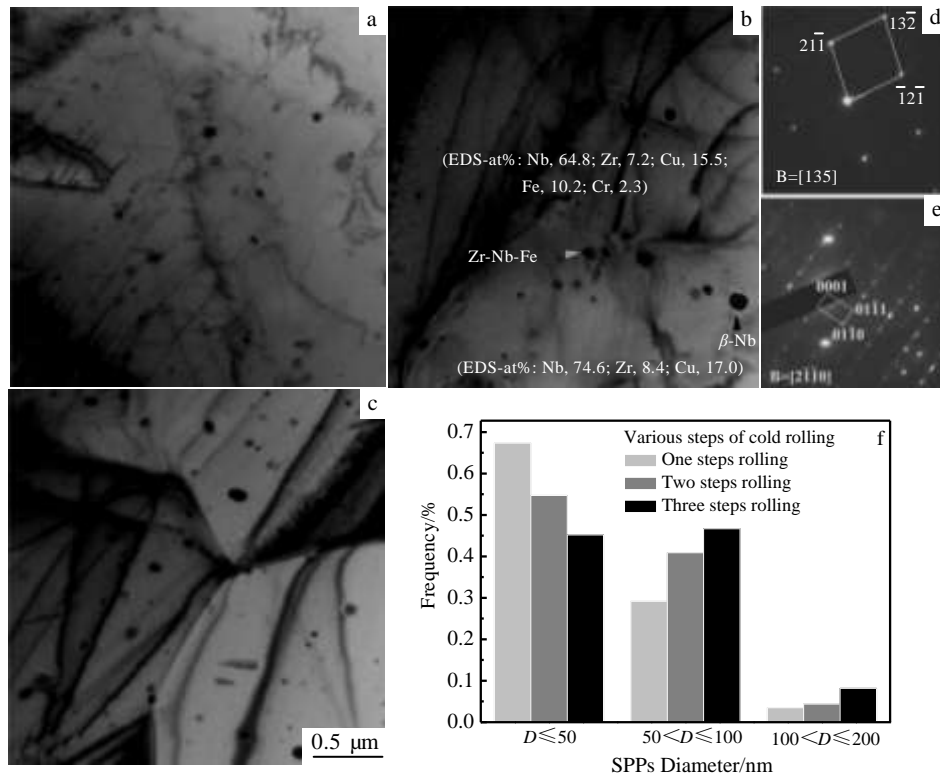


Fig.2 TEM bright-field images and EDS analysis result of the alloy prepared by various cold rolling steps: (a) 2 step, (b) 3 step, and (c) 4 step; (d, e) SAED patterns of β -Nb and Zr-Nb-Fe particles in Fig.2b; (f) the size statistics of SPPs

of Nb in α -Zr is 0.6 wt% at monotectoid temperature of 610 °C in Zr-Nb alloy, and it would decrease to 0.2 wt% if there is small amounts of O or Fe elements in the alloy^[13]. In the present alloy, there is also a little Fe element dissolved in the matrix. Hence, the content of element Nb in the present alloy should be lower than its solubility limits 0.6 wt% and the precipitation of β -Nb phase is promoted.

It can be seen from Fig.2 that with the cold rolling steps increasing from 2 to 4, the morphology and distribution of the SPPs do not change obviously. The morphology of SPPs seems to be spherical, and they disperse homogeneously in the matrix. This is different from the alloys which are hot rolled. Liu et al^[14,15] found that the SPPs in alloys rolled above 780 °C exist in the form of strings and agglomerates.

Fig.2f shows the size statistics of SPPs in the alloy made by various cold rolling steps. It can be seen that with the rolling steps increasing, the frequency of SPPs decreases in the size range smaller than 50 nm, and it increases when the particle size is larger than 50 nm. The result is contrary to some researches, which indicate that with the rolling steps increasing, the size of SPPs in the alloy decrease accordingly due to the particles breaking^[16,17]. In the present study, the difference between various processing is that the total intermediate annealing time increases from 1 h to 3 h, and this is one of the factors which affect the growth

of SPPs. As a result, particles grow with the total annealing time increasing accordingly. Studies show that the precipitation behavior of SPPs is influenced seriously by the final cold rolling reduction before final annealing treatment in zirconium alloys^[18-21]. In the present investigation, the final rolling reduction is 82%, 65%, and 53%. There are more defects in the alloy with large deformation, and nucleation of SPPs is promoted by these defects. The nuclei of SPPs with large numbers would grow slowly because of limited solute atoms in the alloy. So with the increasing of rolling steps, the frequency of the particles smaller than 50 nm decreases accordingly.

2.2 Effect of intermediate annealing temperatures on SPPs precipitation behavior

Fig.3 presents the TEM analyses of Zr-1Nb-0.01Cu alloy annealed at different intermediate annealing temperatures (520, 580, 640 and 700 °C) for 1 h. To avoid repeating work, the processing of Fig.3b annealed at 580 °C is the same as that of Fig.2b (Table 1). When the alloy is annealed at intermediate temperatures 520 and 580 °C (Fig.3a, 3b), only β -Nb and Zr-Nb-Fe can be found in the alloy; when the alloy is annealed at intermediate temperatures 640 and 700 °C, β -Zr (the black big particles) is formed at the grain boundaries (Fig.3c, 3d, 3e). It can be seen that most of β -Zr particles are distributed at the grain boundaries. The

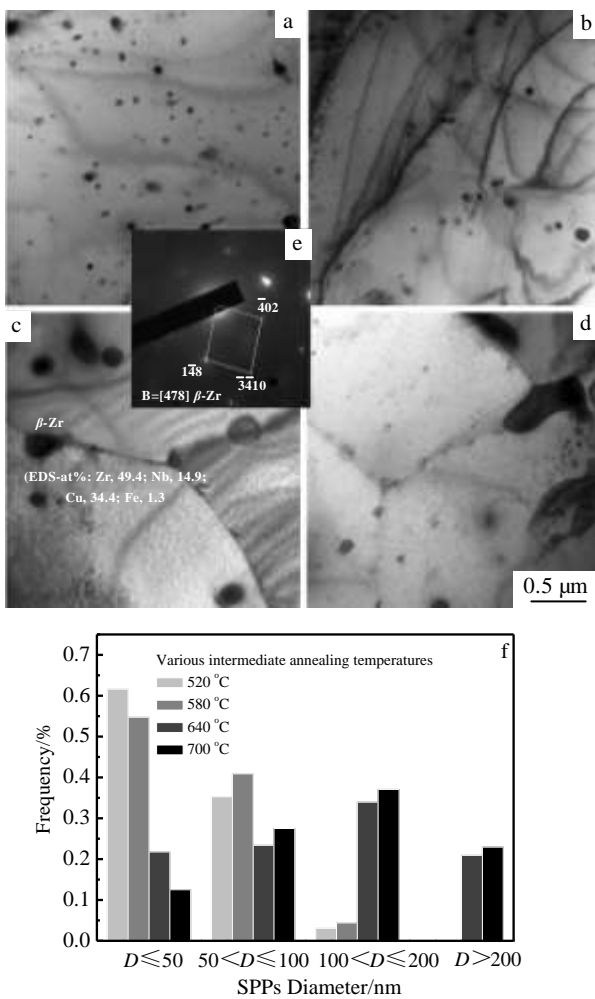


Fig.3 TEM bright-field images of the alloy annealed at different temperatures for 1 h: (a) 520 °C, (b) 580 °C, (c) 640 °C, and (d) 700 °C; (e) SAED pattern of β -Zr in Fig.3c; (f) the size statistics of SPPs

number of β -Nb and Zr-Nb-Fe particles decreases obviously compared with the alloy annealed at intermediate temperatures below 580 °C. Although the alloy has been finally annealed at 560 °C for 4 h, β -Zr is hard to dissolve in the matrix during the subsequent final annealing process and β -Zr is much bigger than β -Nb.

Fig.3f shows the size statistics of SPPs in the alloy at various intermediate annealing temperatures, and the size of β -Zr particles in the alloy was also calculated. It shows that with the temperatures increasing, the frequency of SPPs decreases in the particle size range smaller than 50 nm. When the particle size range is above 100 nm and the temperature is higher than 640 °C, the frequency of SPPs increases obviously due to β -Zr formation.

The distribution of SPPs in zirconium alloys is closely related to the microstructures. The SPPs like β -Nb, Zr-Nb-Fe usually precipitate at the martensite grain boundaries^[19], they usually distribute homogeneously in the matrix with equiaxed

grain structure, and β -Zr generally precipitate at grain boundaries in the alloys with martensite or equiaxed structure^[20]. Researches indicate that the decomposition of β -Zr is affected by chemical composition of zirconium alloys^[4,15,19]. It shows that β -Zr cannot dissolve in the matrix even after 50 h of annealing at 570 °C in Zr-xNb ($x = 0.1\% \sim 2.0\%$) alloys^[4]. But for Zr-Sn-Nb-Fe-Cr alloy^[20], β -Zr dissolves into the matrix when the quenched alloy is annealed at 570 °C for only 1 h, and it also leads to the formation of SPPs (Zr-Nb-Fe) which distributes like band^[15,21].

2.3 Effect of final annealing processes on SPPs precipitation

TEM microstructures of Zr-Nb-Cu alloy prepared at various final annealing temperatures are shown in Fig.4 (the figures of Fig.4c and Fig.2b are the same). With the final annealing temperatures rising from 460 °C to 640 °C, the size of SPPs grows accordingly. When the final annealing temperature is below 610 °C, β -Nb is the main phase precipitated in Zr-Nb-Cu alloy, and a few Zr-Nb-Fe particles also exist in the matrix. As the final annealing temperature is 640 °C, large particles are identified as β -Zr precipitate (Fig.4d) in the alloy and their size is almost 1 μ m. However, the amount of β -Zr phase with the final annealing temperature is less than that of the alloy with the intermediate annealing temperatures of 640 and 700 °C (Fig.4c, 4d). It can be known from Fig.1 and Table. 1 that the alloy intermediate annealed at 640 °C was cold rolled for twice, and the other one final annealed at 640 °C was cold rolled for only once. Study has demonstrated by Chai et al that the pre-deformation before annealing is more effective than prolonging the annealing time in accelerating the phase precipitation^[18]. So it may be the main reason that the amount of β -Zr intermediate annealed at 640 °C is larger than that of the alloy finally annealed at 640 °C. Similar to previous results (Fig.3c and 3d), the precipitations of β -Nb and Zr-Nb-Fe are also suppressed by the formation of β -Zr.

Fig.4e shows the size statistics of SPPs in Zr-1Nb-0.01Cu alloy prepared at different final annealing temperatures. It can be seen that the frequency of the SPPs in the size range 0~50 nm decreases with the temperature increasing. Within the size range from 50 nm to 100 nm, the frequency increases with the increasing temperatures and then decreases at the temperature of 640 °C. When the size range is higher than 100 nm, the frequency rises with temperature increasing, and it increases obviously at 640 °C due to β -Zr formation. There is only β -Zr larger than 200 nm in the alloy.

Fig.5 shows the morphologies of SPPs in the alloy prepared with different final annealing time (the Fig.5b is the same as Fig.2b). The SPPs grow with the increasing final annealing time from 2 h to 8 h. It is obvious that the small particles disappear gradually during the long time annealing process. When the final annealing time is 8 h, the

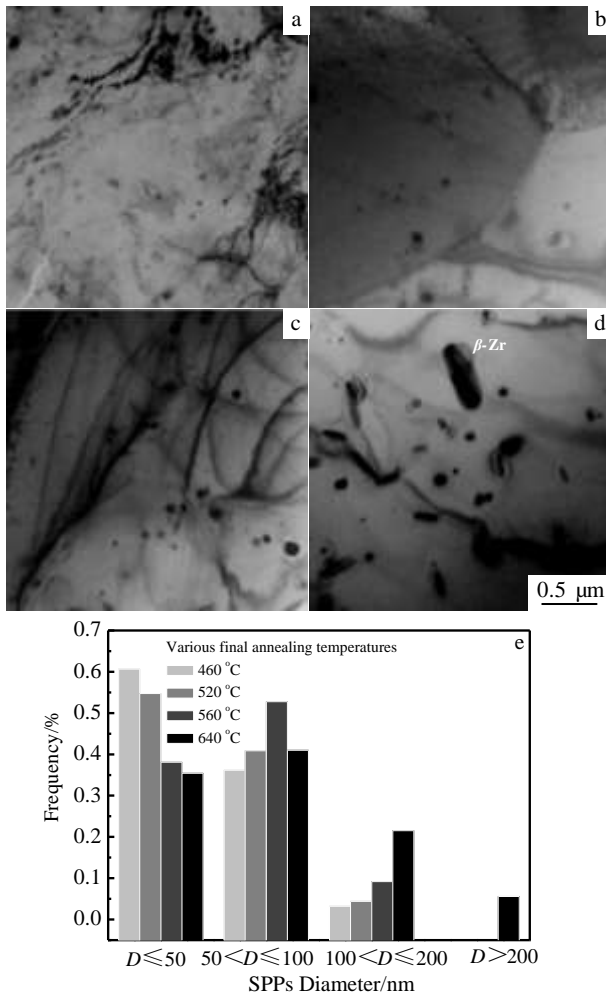


Fig.4 TEM bright-field image of Zr-1Nb-0.01Cu alloy annealed at different temperatures: (a) 460 °C, (b) 520 °C, (c) 560 °C, and (d) 640 °C; (e) the size statistics of SPPs

number of SPPs with the size smaller than 50 nm decrease significantly compared to that annealed for 2 h (Fig.5a and 5d). The reason is that as the annealing proceeds with prolonged time, smaller secondary particles (especially <50 nm) coalesce into larger particles by diffusion through matrix due to Ostwald ripening mechanism^[3]. The size statistics of SPPs (Fig.5e) show that the frequency of the SPPs within 50 nm decreases with increasing annealing time, and it increases with increasing annealing time when the particle size range is higher than 50 nm.

2.4 Comparison of the effects of various processing techniques on SPPs precipitation behavior

The characteristic of SPPs in zirconium alloys is usually described as types, morphology, distribution, particle size, et al. From the analyses above, the precipitation behavior of SPPs is affected obviously by the manufacturing crafts such as intermediate/final annealing temperature and time, rolling steps and final cold rolling reduction. It is well known that

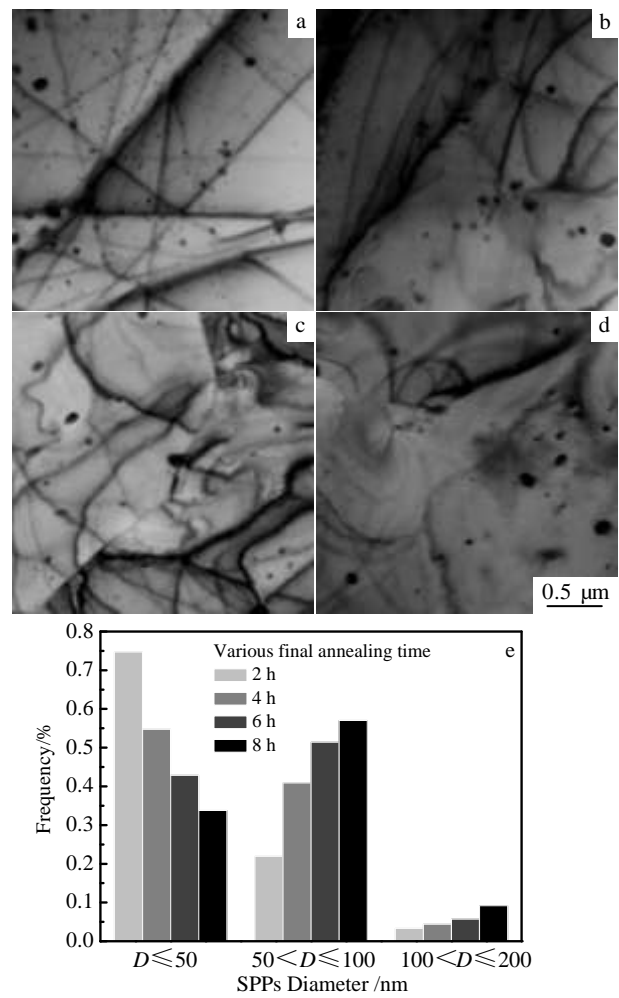


Fig.5 TEM microstructures of Zr-1Nb-0.01Cu alloy prepared with various final annealing time: (a) 2 h, (b) 4 h, (c) 6 h, and (d) 8 h; (e) the size statistics of SPPs

the types of SPPs are closely related to the annealing temperatures in the given alloy^[3,21]. In the present Zr-1Nb-0.01Cu alloys, β-Nb and Zr-Nb-Fe are found in all the alloys by different processing techniques, however, β-Zr only exists when the annealing temperature is above 610 °C. The morphology and the distribution of SPPs in various alloys are almost the same. The most important difference is the particle size, which is also very meaningful for corrosion resistance properties^[22].

Fig.6 shows the effect of various processing techniques on the average size of SPPs in Zr-1Nb-0.01Cu alloy, and the hollow cubic blocks in Fig.6a represent the same manufacturing processing. It can be seen that the techniques have obvious influences on the average size of SPPs, and the size decreases with the decreasing rolling steps, intermediate/final annealing temperatures and time. When the intermediate annealing temperature is higher than 640 °C, the average size of particles becomes very large due to β-Zr

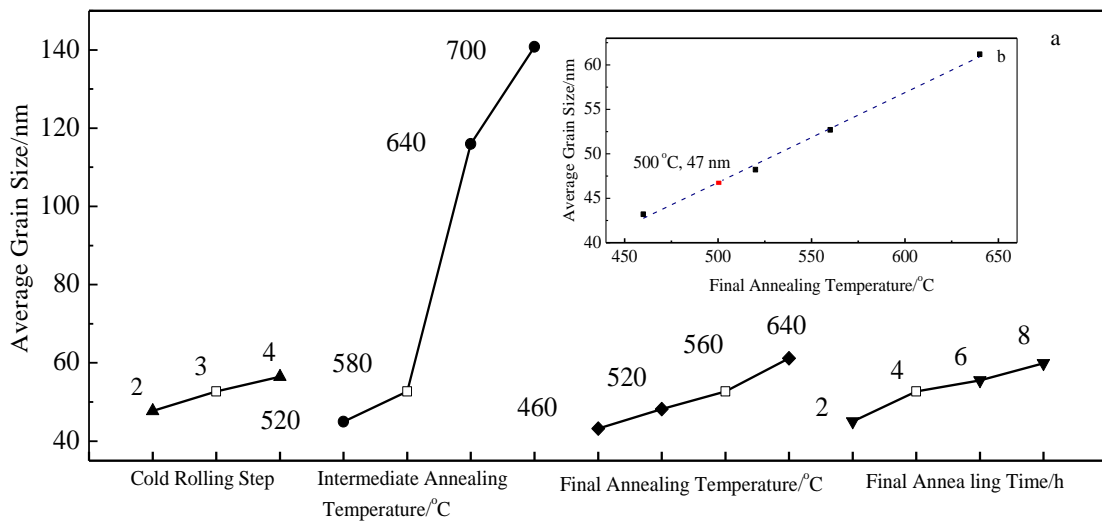


Fig.6 Average size of SPPs in Zr-1Nb-0.05Cu alloys by various processing techniques (a); the relationship between final annealing temperature and average size of SPPs (b)

precipitation. When the intermediate temperature is lower than 580 °C, only β -Nb and Zr-Nb-Fe phases precipitate and the average size is lower than 60 nm. The minimum size of SPPs in the alloy which is final annealed at 460 °C for 4 h is about 43 nm. Although the average particle size can be reduced by increasing rolling reduction before final annealing treatment, it is difficult to be applied in the industrial manufacturing process because of its large deformation. The short time annealing can also limit the growth of SPPs; however, it should be long enough to make sure that the recrystallization of the matrix is totally completed. The most efficient way to reduce the size of SPPs is decreasing annealing temperature. When the intermediate annealing temperature decreases from 580 °C to 520 °C (the difference is 60 °C), the average particle size reduces from 52.7 nm to 45 nm. If the final annealing temperature decreases from 560 °C to 500 °C (the difference is also 60 °C), the size would drop from 52.7 nm to 47 nm, and the average particle size of the alloy final annealed at 500 °C is achieved according to the linear fitting between final annealing temperature and average particle size (Fig.6b). So the decreasing of intermediate annealing temperature seems a bit more efficient in reducing average particle size than the final annealing temperature. Fig.6 also shows that the average particle size smaller than 50 nm can be achieved in the alloy treated at the annealing temperature below 520 °C or for less than 2 h.

The above analysis results are very meaningful for the SPPs control in Zr-Nb based alloys. It is well known that the corrosion behavior of Zr-Nb based alloy is affected obviously by the SPPs precipitation behavior, and it can be improved by the SPPs with small size^[10,15]. According to Fig.6, to get a proper microstructure for improving

corrosion-resistance of zirconium alloys, it is suggested that low annealing temperature (below 520 °C) and short annealing time (about 2 h) should be adopted in the manufacturing process.

3 Conclusions

- 1) The average size of SPPs which contain β -Nb, Zr-Nb-Fe (may contain β -Zr) decreases with the decreasing cold rolling steps, intermediate/final annealing temperature, and annealing time. The decreasing of intermediate annealing temperature is more effective in minimizing the average size of SPPs than the other processing techniques.
- 2) It is hard for β -Zr formed during intermediate annealing process to dissolve in the matrix after final annealing treatment. The SPPs with smaller size coalesce into larger particles by diffusion through matrix gradually because of Ostwald ripening mechanism.
- 3) To acquire proper microstructure with small size of SPPs, it is suggested that low intermediate/final annealing temperature and the short annealing time should be adopted rather than decreasing rolling steps during the manufacturing process of the alloy.

References

- 1 Alam T, Khan M K, Pathak M et al. *Nuclear Engineering and Design*[J], 2011, 241(9): 3658
- 2 Liu W Q, Li Q, Zhou B X et al. *Journal of Nuclear Materials*[J], 2005, 341(2-3): 97
- 3 Luan B F, Chai L J, Chen J W et al. *Journal of Nuclear Materials*[J], 2012, 423(1-3): 127
- 4 Kim H G, Jeong Y H, Kim T H. *Journal of Nuclear Materials*[J], 2004, 326(2-3):125
- 5 Li Z K, Zhou L, Liu J Z et al. *Materials Science and*

- Engineering[J], 2000, 18(S1): 119 (in Chinese)
- 6 Mardon J P, Charquet D, Senevat J. *Zirconium in the Nuclear industry: Twelfth International Symposium*[C]. Toronto, Canada: ASTM STP Press, 1998: 505
- 7 Massih A R, Andersson T, Witt P et al. *Journal of Nuclear Materials*[J], 2003, 322(2-3): 138
- 8 Kim H G, Choi B K, Park J Y et al. *Corrosion Science*[J], 2009, 51(10): 2400
- 9 Jeong Y H, Park S Y, Lee M H et al. *Journal of Nuclear Science and Technology*[J], 2006, 43(9): 977
- 10 Gros J P, Wadier J F. *Journal of Nuclear Materials*[J], 1990, 172(1): 85
- 11 Loucif K, Borrelly R, Merle P. *Journal of Nuclear Materials*[J], 1994, 210(1-2): 84
- 12 Li Q, Liu W Q, Zhou B X. *Rare Metal Materials and Engineering*[J], 2002, 31(5): 389 (in Chinese)
- 13 Woo T, Griffiths M. *Journal of Nuclear Materials*[J], 2009, 384(1): 77
- 14 Liu Y Z, Zhao W J, Peng Q et al. *Materials Chemistry and Physics*[J], 2008, 107(2-3): 534
- 15 Lei M, Liu W Q, Yan Q S et al. *Rare Metal Materials and Engineering*[J], 2007, 36(3): 104 (in Chinese)
- 16 Hallberg H. *International Journal of Mechanical Sciences*[J], 2013, 66: 260
- 17 Ding H T, Shen H G, Shin Y C. *Journal of Materials Processing Technology*[J], 2012, 212(5): 1003
- 18 Chai L J, Luan B F, Chen J W et al. *Acta Metallurgica Sinica*[J], 2012, 48(1): 107 (in Chinese)
- 19 Chai L J, Luan B F, Gao S S et al. *Journal of Nuclear Materials*[J], 2012, 427(1-3): 274
- 20 Kim H G, Kim I H, Choi B K et al. *Corrosion Science*[J], 2010, 52(10): 3162
- 21 Yan Q S, Liu W Q, Lei M et al. *Rare Metal Materials and Engineering*[J], 2007, 36(1): 104 (in Chinese)
- 22 Park J Y, Choi B K, Yoo S J et al. *Journal of Nuclear Materials*[J], 2006, 359: 59

加工工艺对 Zr-1Nb-0.01Cu 合金第二相粒子析出行为的影响

柏广海^{1,2}, 王荣山¹, 张晏玮¹, 梅金娜¹, 李金山², 薛祥义²

(1. 苏州热工研究院有限公司, 江苏 苏州 215004)

(2. 西北工业大学 凝固技术国家重点实验室, 陕西 西安 710072)

摘要: 系统地研究了不同加工工艺对 Zr-1Nb-0.01Cu 合金第二相粒子析出行为的影响。结果表明, 随着冷轧和退火次数减少、中间退火温度和最终退火温度降低与时间的缩短, 第二相粒子的平均晶粒尺寸在减小。在温度高于 640 °C 的中间退火过程中形成的 β -Zr 相在最终的退火过程中很难完全分解。由于 Ostwald 熟化效应, 最终退火时间的延长会导致合金中尺寸较小的第二相粒子通过原子扩散合并成尺寸较大的第二相粒子。与其它加工工艺相比, 降低中间退火温度在减小第二相粒子尺寸方面更为有效。通过低温中间/最终退火 (≤ 520 °C) 或缩短退火时间 (≤ 2 h) 可获得平均晶粒尺寸小于 50 nm 的第二相粒子。研究结果对调控 Zr-Nb 系合金第二相粒子的析出行为具有重要意义。

关键词: Zr-1Nb-0.01Cu 合金; 加工工艺; 第二相粒子; 析出行为; 晶粒尺寸

作者简介: 柏广海, 男, 1981 年生, 博士后, 苏州热工研究院有限公司寿命管理技术中心, 江苏 苏州 215004, 电话: 0512-68701561,

E-mail: baiguanghai@foxmail.com